

Conference Paper

A possibility of detecting fast neutrons in a ^{10}B solid-gas detector

S Potashev¹, Yu Burmistrov¹, A Drachev², S Karaevsky¹, E Konobeevski¹, A Kasparov¹, I Meshkov³, S Zuyev¹, A Afonin¹, V Marin¹, V Ponomarev¹, and G Solodukhov¹

¹Institute for Nuclear Research, Russian Academy of Sciences, 117312, Moscow, Russia

²State Research Institute for Chemistry and Technology of Organoelement Compounds, 105118, Moscow, Russia

³Lebedev Physical Institute, Russian Academy of Sciences, 119991, Moscow, Russia

Abstract

The possibility of detecting thermal and fast neutrons in ^{10}B solid-gas detector is considered. The simulation of the neutron detection process shows a significant difference in the detector signals caused by neutrons of different energies. An experimental verification of the detector's operation was performed using W-Be photoneutron source with different ratio of fast and thermal neutrons incident on the detector. The measured amplitude spectra of the signals for different neutron energies were compared with the simulation results. The qualitative agreement between experimental and calculated data indicates the possibility of using this detector for recording thermal and fast neutrons.

Corresponding Author:

S Potashev
 potashev@inr.ru

Received: 25 December 2017

Accepted: 2 February 2018

Published: 9 April 2018

Publishing services provided by
 Knowledge E

© S Potashev et al. This article is distributed under the terms of the [Creative Commons](#)

[Attribution License](#), which permits unrestricted use and redistribution provided that the original author and source are credited.

Selection and Peer-review under the responsibility of the ICPPA Conference Committee.

1. Introduction

To perform experiments using the Photoneutron source at the Institute for Nuclear Research of the Russian Academy of Sciences it is important to determine the contributions of thermal and fast neutrons during the irradiation. Most neutron detectors, such as gas counters and ^3He -proportional chambers are designed for registration of thermal neutrons. Recently, new position-sensitive neutron detectors (PSNDs) with solid layers containing ^{10}B have been created. They are hybrid detectors [1-3], which contain ^{10}B layer used as a converter of neutron into charged particles which are detected in a gas-discharge chamber. The advantage of such detectors to detectors with helium-3 is an ability to operate in a wide range of neutron energies. The localization of the neutron interaction point in the layer plane and the small gas gap provide a high spatial resolution. These detectors may operate using cheap gases at atmospheric pressure.

In this paper, we consider a hybrid position-sensitive detector based on the solid ^{10}B layer and a proportional chamber with sensitive dimensions of 100x100 mm² [4].

OPEN ACCESS

Its geometry with two 2-mm gas gaps and rather low neutron detection efficiency is suitable for detecting not only intense thermal fluxes but also the fast neutron ones. This detector has been used now at the Photoneutron source of INR RAS.

2. Experimental Scheme

W-Be photoneutron source of INR is installed at the electron beam of LUE-8-5 linear accelerator. A beam of electrons is incident on a tungsten bremsstrahlung target. Bremsstrahlung photons from the target generate a neutrons in a beryllium photoneutron target. The neutron source has output neutron and can be used in different configurations. The configuration I of the source ensures the enrichment of the neutron spectrum by thermal neutrons due to a thermalization of in the moderator. The configuration II is intended for enrichment of the spectrum by fast neutrons. The PSND was located at the exit from the source channel at a distance of 210 cm from the center of the source.

The principle of neutron detection in PSND is illustrated by the scheme shown in Figure 1. The ^{10}B nucleus captures a neutron and forms the nucleus $^{11}\text{B}^*$ in the excited state, which decays as shown below:

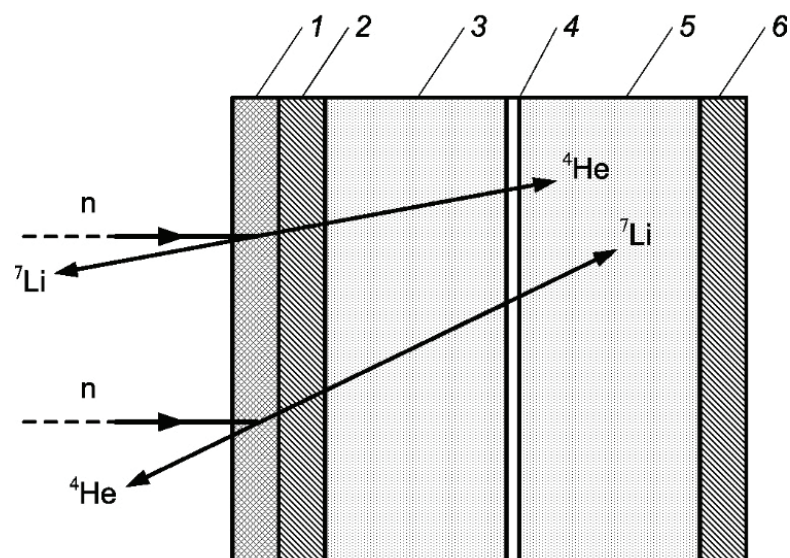
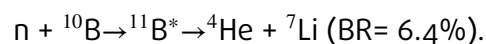
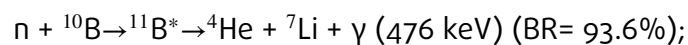


Figure 1: Scheme of neutron detection in PSND: 1 - 3 μm ^{10}B layer; 2 - cathode 0.2 μm Al layer; 3 - 2 mm first gas gap; 4 - anode of parallel wires with 2 mm step - X coordinate; 5 - 2 mm second gas gap; 6 - cathode of parallel strips with 2 mm step - Y coordinate.

For thermal neutrons ${}^4\text{He}$ and ${}^7\text{Li}$ nuclei are emitted in opposite directions. In each interaction act the detector, as shown in Figure 1, can detect only one nucleus. If a

TABLE 1: The ranges R and the corresponding relative fractions P of ^4He and ^7Li in the layer of boron, aluminum and in the total gas gap of the detector.

n	^4He				^7Li			
	E (MeV)	R in ^{10}B (μm)	R in $^{40}\text{Ar}+\text{C}_4\text{H}_8$ (mm)	P (%)	E_{Li} (MeV)	R_{Li} in ^{10}B (μm)	R_{Li} in $^{40}\text{Ar}+\text{C}_4\text{H}_8$ (mm)	P (%)
Thermal	1.5	3.3	9	> 99	0.8	1.6	4	< 1
1	1.5 – 2.8	3.3 – 7.2	9 – 18.4	90	0.7 – 1.9	1.4 – 2.9	4 – 7.8	10
2	2.1 – 4.6	5 – 14.5	13 – 36.1	75	0.9 – 3.2	1.7 – 4.6	4.7 – 11.5	25
3	2.8 – 6.4	7.2 – 24.2	18.4 – 59.1	60	1 – 4.6	1.8 – 6.6	5 – 16	40

neutron has energy of several MeV, it can transfer its kinetic energy to the registered nucleus. The trigger signal for the neutron detection event occurs only if the ionization losses in the second gas gap exceed the set threshold. Only events which caused the ionization losses signal in both gas gaps are selected. All the wires of the anode and all cathode strips are electrically connected to one another through the same resistances. The amplitudes of the coordinate signals X_1 , X_2 and Y_1 , Y_2 from the two ends of the resistance circuits of wires and strips are fed to the corresponding forming amplifiers. When the trigger signal arrives, all four amplitudes of the coordinate signals are encoded and form a neutron detection event.

3. Simulation of ionization losses in a detector

A kinematic simulation of the $n + ^{10}\text{B} \rightarrow ^4\text{He} + ^7\text{Li} + \gamma$ (476 keV) reaction was carried out. For thermal neutrons, the secondary charged particles ^4He and ^7Li are emitted at opening angle of 180° , which leads to the detection of either lithium or helium. The kinetic energy of ^4He is about of 1.47 MeV, and that of ^7Li - 0.84 MeV. The table 1 shows the ranges R of ^4He and ^7Li in the layer of boron, aluminum and in the total gas gap of the detector and the corresponding relative fractions P of ^4He and ^7Li in the number of events recorded by the detector for different neutron energies.

Simulation shows that at thermal neutron energies, basically the events from ^4He detection will be observed, as the fraction of ^7Li particles entering the second gas will be less than 1% of all recorded particles. At neutron energies greater than 1 MeV, ionization loss pulses from both ^4He and ^7Li nuclei can occur in both gas gaps.

In Figure 2 the simulated spectra of ionization losses in the total gas gap of the PSND caused by thermal neutrons and neutrons with energies of 1, 3, and 5 MeV are shown. For thermal neutrons, the signal is mainly determined by ionization losses of ^4He . The

maximum in the thermal spectrum corresponds to ionization losses of 0.85 MeV. At energy of 1 MeV and higher, one can see a contribution of ^7Li nuclei to the spectra. In this case, the small amplitudes in the spectrum basically correspond to the ^4He losses, and the large amplitudes are mainly associated with the ^7Li losses. The right-hand boundary of the spectrum depends on the maximum energy in the neutron spectrum.

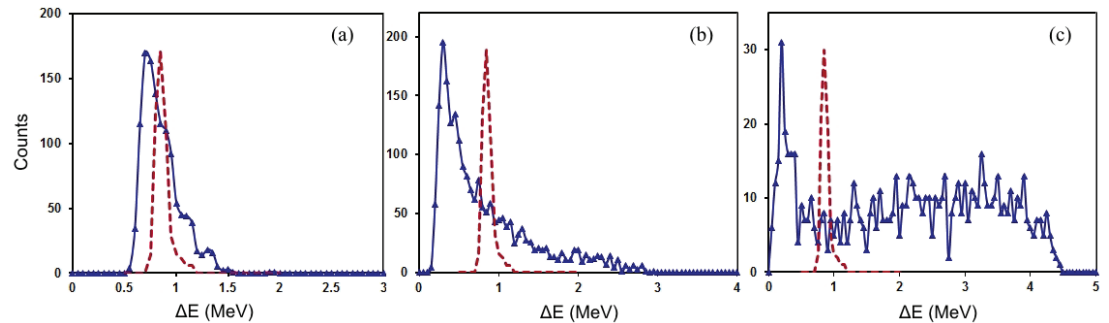


Figure 2: Simulated energy loss spectra in the total gas gap for neutron energy of 1 MeV (a); 3 MeV (b) and 5 MeV (c). A dashed line shows the loss spectra for thermal neutrons.

4. Experimental energy losses for different neutron source configuration

The experiments were performed at electron energy of 7 MeV. In configuration I, the neutron flux was enriched by thermal neutrons. The cadmium mask of 1 mm thick, installed in the front of the PSND, allowed to reduce the thermal detector neutron load, the efficiency of which is much greater than that for fast neutrons. The measured amplitude spectra for the total gaps shown in Figure 3 are close in shape to the calculated spectra. The deviation of experimental losses from the calculated ones indicates a possible presence of fast neutron in the neutron flux in configuration I.

In configuration II, the flux is enriched by fast neutrons in comparison with the thermal ones. In this configuration, in contrast to configuration I, the data must contain events from neutrons with MeV energy. Figure 4 shows the energy loss spectra in the total gas gap of the PSND for the source configuration II. The shape of the spectrum in Figure 3 corresponds most closely to the calculated spectrum for thermal neutrons in Figure 2. The shape of the spectrum in Figure 4 corresponds most closely to the calculated spectrum in Figure 2 (b). This corresponds to the most probable neutron energy of about 3 MeV. At such energy the ^7Li nucleus may obtain enough energy to be registered in the PBNB and produce large ionization losses. Comparison of Figure 3 and 4 indicates also the presence of thermal neutrons in both source configurations..

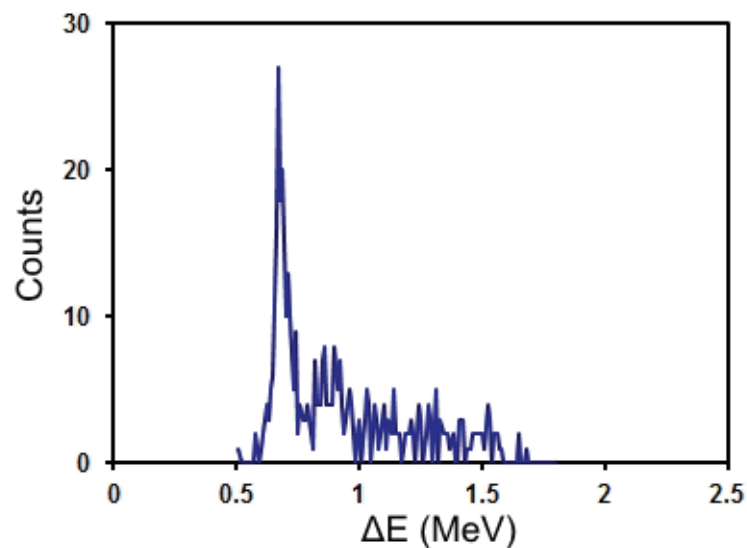


Figure 3: Spectra of energy losses in the total gas gap for the source configuration I.

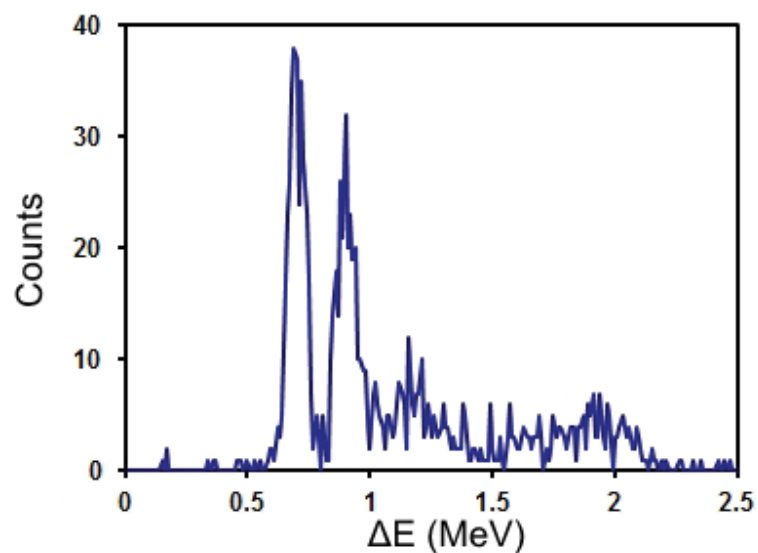


Figure 4: Spectra of energy losses in the total gas gap for the source configuration II.

5. Conclusion

The process of detecting thermal and fast neutrons in ^{10}B solid-gas detector is considered. The simulation of the neutron detection shows a significant difference in the detector signals caused by neutrons of different energies. An experimental verification of the detector's operation was performed using W-Be photoneutron source with different ratio of fast and thermal neutrons incident on the detector. The measured amplitude spectra of the signals for different neutron energies were compared with the simulation results. The qualitative agreement between experimental and calculated

data indicates the possibility of using this detector for recording thermal and fast neutrons.

References

- [1] Köhli M, Allmendinger F, Häußler W et al. 2016 *Nucl. Instr. and Meth. A* **828** 242
- [2] Uno S, Uchida T, Sekimoto M et al. 2012 *Phys. Procedia* **26** 142
- [3] Piscitelli F et al. 2017 *J. of Instr.* **12** P03013
- [4] Potashev S, Burmistrov Yu, Drachev A, Karaevsky S, Konobeevski E and Zuyev S 2017 *J. Phys.: Conf. Ser.* **798** 012160